

Longitudinal Plasma Motions Generated by Shear Alfvén Waves in Plasma with Thermal Misbalance

S. Belov^{1,2} · S. Vasheghani Farahani³ ·
N. Molevich^{1,2} · D. Zavershinskii^{1,2}

© Springer

Abstract Compressional plasma perturbations may cause thermal misbalance between plasma heating and cooling processes. This misbalance significantly affects the dispersion properties of compressional waves providing a feedback between the perturbations and plasmas. It has been shown that Alfvén waves may induce longitudinal (compressional) plasma motions. In the present study, we analyze the effects of thermal misbalance caused by longitudinal plasma motions induced by shear Alfvén waves. We show that thermal misbalance leads to appearance of exponential bulk flows, which itself modifies the Alfvén-induced plasma motions. In the case of sinusoidal Alfvén waves, we show how the amplitude and phase shift of induced longitudinal motions gain dependence on the Alfvén wave frequency while shedding light on its functionality. This feature has been investigated analytically in application to coronal conditions. We also consider the evolution of longitudinal plasma motions induced by the shear sinusoidal Alfvén wave by numerical methods before comparing the results obtained with our presented analytical predictions to justify the model under consideration in the present study.

Keywords: Waves, Alfvén; Magnetohydrodynamics; Coronal Seismology

1. Introduction

A perfect domain in physics to study the character of Alfvén waves together with their seismological aspects is the Sun. This statement is not just supported

✉ S.A. Belov
mr_beloff@mail.ru

¹ Department of Physics, Samara National Research University, Moscovskoe sh. 34, Samara, 443086, Russia

² Department of Theoretical Physics, Lebedev Physical Institute, Novo-Sadovaya st. 221, Samara, 443011, Russia

³ Department of Physics, Tafresh University, Tafresh 39518 79611, Iran

by the knowledge that the Alfvén wave is the primary candidate for carrying energy from the lower to outer solar atmosphere, but benefits from the Alfvén-wave contribution towards understanding coronal heating. An important feature of the Alfvén wave that is of interest in the present study is rooted in its nature since its presence is associated with the magnetic-tension force (Alfvén, 1942).

The magnetic-tension force is one of the main nonlinear forces connected with the Alfvén wave (Vasheghani Farahani, S. et al., 2011) that affects the compressive perturbations in a plasma medium. This is in the sense that the interplay of these forces in a transversely structured plasma structure provides cylindrical collimation through the compressive perturbations, especially the longitudinal perturbations, owing to the Bernoulli effect (Vasheghani Farahani and Hejazi, 2017). A prominent nonlinear force in this regard is the ponderomotive force (Verwichte, Nakariakov, and Longbottom, 1999), which in specific ideal conditions acts as the only force that sustains jet collimation (Mozafari Ghoraba and Vasheghani Farahani, 2018). Even in the absence of transverse structuring in a uniform plasma medium that hosts a magnetic null-point (Prokopyshyn, Hood, and De Moortel, 2019), the ponderomotive force connected with the Alfvén wave induces longitudinal, together with transverse magnetoacoustic, waves that contribute towards energy transfer in the solar atmosphere (Sabri et al., 2018). The back reaction of the density perturbations together with the longitudinal induced flows initiated by the ponderomotive force on the initially propagating Alfvén wave creates a non-uniform background in the medium (Sabri et al., 2020). This non-uniformity would act as if the plasma were initially inhomogeneous, which results in a famous physical concept known as phase mixing (Thurgood and McLaughlin, 2013), which itself is a damping mechanism (Nakariakov, Roberts, and Murawski, 1997; Craig and Fruit, 2005; Ruderman and Petrukhin, 2018). Regarding a visco-resistive medium with inhomogeneous plasma density, the induced longitudinal flows due to the ponderomotive force provide local temperature increases that trigger longitudinal flows in the context of phase mixing (McLaughlin, de Moortel, and Hood, 2011; Shestov et al., 2017).

The solar corona makes the interplay between magnetic and compressional perturbations even more intriguing. Temperature and/or density variations caused by magnetoacoustic (MA) waves or induced by magnetic perturbations disturb the balance between plasma heating and radiative-cooling rates allowing the thermal-misbalance effect (Field, 1965; Molevich and Oraevskii, 1988; Nakariakov et al., 2017) to develop. The origin of thermal misbalance comes from the dependence of coronal heating together with the cooling rates on plasma parameters such as density and temperature. The changes of rates due to compression affect the variations, which results in re-establishing the interplay between plasma-heating/cooling processes and compressional perturbation. Thus, the interplay between magnetic perturbations/forces and non-adiabatic processes via compression variations can be established as well. This non-linear effect is the subject of the current research.

The thermal misbalance significantly affects the dispersion properties of compressional eigenmode leading to mode amplification/damping, frequency dependence of the phase speed, and increment/decrement (Zavershinskii et al., 2019; Molevich and Oraevskii, 1988) and a number of effects visible on either

linear and non-linear stages of wave evolution (see Chin et al., 2010; Nakariakov et al., 2017; Claes and Keppens, 2019; Zavershinskii et al., 2020; Antolin, 2020, etc.). Interestingly, the temporal scales determining properties of compressional perturbations are the scales in which the cooling/heating misbalance function depends on the plasma parameters (see Zavershinskii et al., 2019, for details) not the cooling or heating timescales. It has been shown that these timescales are of the same order as observed MA waves and oscillations (Zavershinskii et al., 2019; Kolotkov, Nakariakov, and Zavershinskii, 2019). Analysis conducted by Kolotkov, Nakariakov, and Zavershinskii (2019) showed that a reasonable choice of the unspecified coronal-heating function allows one to reproduce the observed properties of standing slow MA oscillations. Subsequently, Kolotkov, Duckenfield, and Nakariakov (2020) seismologically constrained the coronal-heating function using observations of slow MA waves in various coronal-plasma structures. Considering some specific mechanisms satisfying seismological constraints, Prasad, Srivastava, and Wang (2021) revealed that inclusion of thermal misbalance in addition to thermal conductivity and compressive viscosity better matches the predicted scaling law between the damping time and wave period for the observed *Solar Ultraviolet Measurements of Emitted Radiation* (SUMER) oscillations. Regarding the propagation of Alfvén waves in a non-ideal plasma medium that resembles coronal holes, the thermal misbalance modifies the wave-steepening scale so that for lower solar atmospheric conditions the Alfvén-wave steepening is strengthened while experiencing either forward or backward shock. However, as for the slow magnetoacoustic waves where either amplification or damping is observed (Nakariakov et al., 2017), the thermal misbalance may either steepen or dampen the amplitude of the Alfvén wave subject to conditions (Belov, Molevich, and Zavershinskii, 2019a, 2020). It is worth stating that Alfvén waves may be bi-exponentially amplified due to parametric interactions with isentropically unstable acoustic/magnetoacoustic waves (Zavershinskiy and Molevich, 2015; Belov, Molevich, and Zavershinskii, 2018, 2019b). However, when transverse structuring exists, torsional Alfvén waves are possible candidates for carrying vast amounts of energy in the lower solar atmosphere contributing towards coronal heating (Srivastava et al., 2017). This is why when transverse structuring is present in the plasma medium, the Alfvén-wave steepening would eventually form a shock that is directly proportional to the equilibrium flow speed that provides a shear at the boundary of the plasma structure (Farahani, Hejazi, and Boroomand, 2021). In addition to shocks, pseudo-shocks also contribute towards energy supply to the inner solar corona providing localized mass transport together with coronal heating (Srivastava et al., 2018).

In the present study, the aim is to shed light on the perturbations induced by shear Alfvén waves in the presence of thermal misbalance by focusing on the nonlinear forces connected with the shear Alfvén wave, where in the succeeding section the model and equilibrium conditions are to be presented. In the third section, expressions governing the induced perturbations are provided before carrying out parametric studies regarding the scaling behavior of the amplitude and phase shift as well as comparison between the analytic solutions and results obtained numerically. In the final section, the conclusions are summarized.

2. Model and Equilibrium Conditions

Consider a fully ionized plasma medium that resembles the solar atmosphere, where due to the macroscopic view of the present study it provides a perfect domain for implementing the MHD theory. In this line the MHD equations are taken under consideration to model the dynamics of Alfvén waves in an initially homogeneous plasma medium that experiences a misbalance between non-adiabatic heating and radiative losses (Priest, 2014). The MHD set of equations appropriate for the aims of the present study are expressed as

$$\frac{\partial \rho}{\partial t} + \nabla \cdot (\rho \mathbf{v}) = 0, \quad (1)$$

$$\rho \left(\frac{\partial \mathbf{v}}{\partial t} + (\mathbf{v} \cdot \nabla) \mathbf{v} \right) = -\nabla P - \frac{1}{4\pi} \mathbf{B} \times (\nabla \times \mathbf{B}), \quad (2)$$

$$\frac{\partial \mathbf{B}}{\partial t} = \nabla \times (\mathbf{v} \times \mathbf{B}), \quad (3)$$

$$\nabla \cdot \mathbf{B} = 0, \quad (4)$$

$$C_{V\infty} \rho \left(\frac{\partial T}{\partial t} + (\mathbf{v} \cdot \nabla) T \right) - \frac{k_B T}{m} \left(\frac{\partial \rho}{\partial t} + (\mathbf{v} \cdot \nabla) \rho \right) = -\rho Q(\rho, T), \quad (5)$$

$$P = \frac{k_B}{m} \rho T, \quad (6)$$

where ρ , T , and P respectively represent the density, temperature, and pressure of the plasma, while \mathbf{v} and \mathbf{B} are vectors of the plasma velocity and magnetic field. The Boltzmann constant, the mean mass per volume, and the high-frequency specific heat capacity at constant volume are respectively shown by k_B , m , and $C_{V\infty}$. The term $Q(\rho, T) = L(\rho, T) - H(\rho, T)$ is the generalized heat-loss function (Parker, 1953; Field, 1965) expressed by the cooling and heating rates represented by $L(\rho, T)$ and $H(\rho, T)$, respectively. It is worth noting that the heat-loss function $Q(\rho, T)$ equals zero under steady-state conditions where we have $Q(\rho_0, T_0) = L(\rho_0, T_0) - H(\rho_0, T_0) = L_0 - H_0 = 0$. As the cooling and heating rates depend on density and temperature, the perturbations of the physical variables initiate the thermal misbalance where the reaction on the wave dynamics is of interest in the present study. Further, we consider a propagating 1D linear polarized shear Alfvén wave polarized in the x -direction propagating along the z -axis in the positive direction parallel to the external magnetic field $B_z = B_0$. In the weakly nonlinear regime, the perturbation theory up to the second order of small parameter $\alpha \ll 1$, $\rho = \rho_0 + \alpha \rho_1 + \alpha^2 \rho_2$ and $B_x = \alpha B_{x1} + \alpha^2 B_{x2}$ is applied to the set of equations expressed by Equations 1–6. By assuming that there are no acoustic perturbations in the first order of α , Equations 1–6 could

be simplified to

$$\begin{aligned} & \frac{\partial}{\partial t} \left(\frac{\partial^2 v_z}{\partial t^2} - C_\infty^2 \frac{\partial^2 v_z}{\partial z^2} + \frac{\partial^2}{\partial z \partial t} \frac{B_x^2}{8\pi\rho_0} \right) + \\ & + \frac{1}{\tau_V} \left(\frac{\partial^2 v_z}{\partial t^2} - C_0^2 \frac{\partial^2 v_z}{\partial z^2} + \frac{\partial^2}{\partial z \partial t} \frac{B_x^2}{8\pi\rho_0} \right) = 0. \end{aligned} \quad (7)$$

$$\frac{\partial^2 B_x}{\partial t^2} - C_A^2 \frac{\partial^2 B_x}{\partial z^2} = 0, \quad (8)$$

where $C_\infty^2 = C_{P\infty} k_B T_0 / C_{V\infty} m$ is the square of high-frequency ($\omega |\tau_V| \gg 1$) sound speed (the standard value of the sound speed in the medium without the thermal misbalance) and $C_0^2 = (Q_{0T} - Q_{0\rho} \rho_0 / T_0) k_B T_0 / Q_{0T} m$ is the square of the low-frequency ($\omega |\tau_V| \ll 1$) sound speed that arises due to the thermal misbalance. The sound speed in the medium under consideration is frequency dependent and varies between C_0 and C_∞ (see, e.g., Molevich and Oraevskii, 1988; Zavershinskii et al., 2019). It is worth stating that in case of non-misbalance conditions, there is no dispersion caused by the heating/cooling processes and acoustic waves propagate with the phase speed C_∞ . Here, also, $C_A^2 = B_0^2 / 4\pi\rho_0$ is the square of Alfvén speed; $C_{P\infty} = C_{V\infty} + k_B/m$ is the high-frequency specific heat capacity at constant pressure; $\tau_V = C_{V\infty} / Q_{0T}$ is the characteristic time associated with the thermal misbalance (see τ_2 in Zavershinskii et al., 2019; Kolotkov, Duckenfield, and Nakariakov, 2020); $Q_{0T} = \partial Q / \partial T|_{\rho_0, T_0}$, $Q_{0\rho} = \partial Q / \partial \rho|_{\rho_0, T_0}$. It should be mentioned that $v_z \propto \alpha^2$ (second-order perturbation), while $B_x \propto \alpha$ (first-order perturbation), so that Equation 7 describes second-order effects.

It can be seen from Equation 7, that the Alfvén wave induces longitudinal plasma motions due to the magnetic pressure $[B_x^2/8\pi]$ gradient. At the same time, Equation 8 has the exact solution in the form of an Alfvén wave propagating in the positive direction in the form of $B_x = \Phi(\xi)$, where we have $\xi = z - C_A t$. Looking for the Alfvén-induced motion, we look for the solution of Equation 7 of the form $v_z = v_z(\xi)$. In this case, Equation 7 may be written as a simple ordinary differential equation

$$\frac{d}{d\xi} \left(C_A (C_\infty^2 - C_A^2) v_z + \frac{C_A^4}{2B_0^2} B_x^2 \right) + \frac{1}{\tau_V} \left((C_A^2 - C_0^2) v_z - \frac{C_A^3}{2B_0^2} B_x^2 \right) = 0. \quad (9)$$

Equation 9 allows us to express v_z as a function of B_x^2 . This solution can be seen from Equation 10, where C is an arbitrary constant determined from the condition $v_z|_{\xi=0} = 0$. Thus, we have

$$\begin{aligned} v_z &= C e^{\Psi\xi} + K_1 B_x^2 + K_2 e^{\Psi\xi} \int e^{-\Psi\xi} B_x^2 d\xi, \\ K_1 &= \frac{C_A^3}{2(C_A^2 - C_\infty^2)B_0^2}, \quad K_2 = \frac{C_A^2 (C_\infty^2 - C_0^2)}{2\tau_V (C_A^2 - C_\infty^2)^2 B_0^2}, \quad \Psi = \frac{(C_A^2 - C_0^2)}{C_A \tau_V (C_A^2 - C_\infty^2)}. \end{aligned} \quad (10)$$

Equation 10 determines longitudinal plasma motions induced by Alfvén waves in a plasma with thermal misbalance. It is worth noting that K_1 and K_2 should

be of the order unity to satisfy the expansion order, which implies, in particular, that $\beta < 1$.

The first term of the solution expressed by Equation 10 is a bulk flow analogous to the bulk flow obtained by McLaughlin, de Moortel, and Hood (2011) for the case of visco-resistive plasma. This flow arises due to the fact that thermal misbalance causes local increase/decrease in temperature, which leads to an increase in the pressure gradients that drives the bulk flow. We should stress specific features following from the consideration of thermal misbalance. In the visco-resistive case, the flow follows the direction of the Alfvén wave. But, in thermally active plasmas, the flow travels either in the direction of the Alfvén wave or opposite to it. In the following section, we will introduce the conditions for same- and opposite- direction flows considering the sinusoidal inducing Alfvén wave.

The second term of the solution expressed by Equation 10 coincides with the Alfvén-induced motion in an ideal plasma without thermal misbalance. The last term of the solution expressed by Equation 10 describes how the thermal misbalance affects the longitudinal plasma motion induced by the Alfvén wave. This influence is as follows: compressional plasma perturbations induced by the magnetic-pressure gradients in the Alfvén wave cause the thermal misbalance, which leads to the additional plasma heating or cooling, similar to the case of bulk flow; see the first term. Subsequently, this disturbed heating/cooling introduces gas-dynamic pressure gradients driving longitudinal-plasma motions. A simple mechanical analogue of this process is driven oscillations of a pendulum with a positive/negative friction. The external force with its own frequency moves a pendulum, but a positive/negative friction leads to the energy dissipation/gain that causes the oscillations to experience a phase-shift. Following this analogy, plasma particles act like a pendulum, the ponderomotive force induced by the Alfvén wave is an external force, and the thermal misbalance acts as some positive/negative friction.

3. Results and Discussions

Let us examine the solution expressed by Equation 10 for the sinusoidal Alfvén wave with relative amplitude $\epsilon \ll 1$:

$$B_x = \epsilon B_0 \sin(k\xi) = \epsilon B_0 \frac{e^{ik\xi} - e^{-ik\xi}}{2i}. \quad (11)$$

Substitute the signal expressed by Equation 11 into the expression expressed by Equation 10) to obtain Equation 12 for the longitudinal plasma velocity with the initial condition $v_z|_{\xi=0} = 0$ as

$$v_z = C e^{\Psi\xi} + V_0 - (A_1 \cos(2k\xi) - A_2 \sin(2k\xi)), \quad (12)$$

where

$$C = \frac{\epsilon^2 C_A^3}{4} \frac{4\omega^2 \tau_V^2 (C_\infty^2 - C_0^2) (C_A^2 - C_\infty^2)}{\left((C_A^2 - C_0^2)^2 + 4\omega^2 \tau_V^2 (C_A^2 - C_\infty^2)^2\right) (C_A^2 - C_0^2)},$$

$$\begin{aligned}
 V_0 &= \frac{\epsilon^2}{4} \frac{C_A^3}{C_A^2 - C_0^2}, \\
 A_1 &= \frac{\epsilon^2 C_A^3}{4} \frac{((C_A^2 - C_0^2) + 4\omega^2 \tau_V^2 (C_A^2 - C_\infty^2))}{(C_A^2 - C_0^2)^2 + 4\omega^2 \tau_V^2 (C_A^2 - C_\infty^2)^2}, \\
 A_2 &= \frac{\epsilon^2 C_A^3}{4} \frac{2\omega \tau_V (C_0^2 - C_\infty^2)}{(C_A^2 - C_0^2)^2 + 4\omega^2 \tau_V^2 (C_A^2 - C_\infty^2)^2},
 \end{aligned}$$

where we have $\omega = C_A k$. Equation 12 may be rewritten in a more convenient form by transformation of the oscillating part as

$$\begin{aligned}
 v_z &= C e^{\Psi \xi} + V_0 - A \cos(2k\xi + \phi_0), \\
 A &= \sqrt{A_1^2 + A_2^2}, \quad \phi_0 = \arctan\left(\frac{A_2}{A_1}\right).
 \end{aligned} \tag{13}$$

In the case without thermal misbalance, the RHS of Equation 13 equals $\epsilon^2 C_A^3 \cdot (1 - \cos(2k\xi)) / 4 (C_A^2 - C_\infty^2)$ which coincides with the expression obtained by McLaughlin, de Moortel, and Hood (2011) for the case of an ideal plasma. The primary feature of the obtained longitudinal motion is the presence of an exponential bulk flow. The direction of this flow is determined by the sign of C (see Equation 12). When we have $C > 0$, the flow is co-directed with the Alfvén wave, and conversely, if we have $C < 0$, the flow is oppositely-directed. For $C_A^2 > C_\infty^2, C_0^2$ (Alfvén waves are faster than acoustic waves), this flow is co-directed if $C_\infty^2 > C_0^2$. For $\tau_V > 0$, this condition coincides with the condition of isentropic stability $\tau_V (C_\infty^2 - C_0^2) > 0$ (see, e.g., Molevich and Oraevskii, 1988; Zavershinskii et al., 2020). Thus, the flow is co-directed with the Alfvén wave in the isentropically stable plasma and oppositely-directed in the isentropically unstable plasma. Note that this direction for flows is similar to those described earlier in the heat-releasing gaseous media when acoustic flows arose against the propagation of the initiating wave in the case of isentropic instability and along the propagation of the initiating wave in the case of stability (Molevich, 2001, 2002). The second feature is that the velocity amplitude A of the oscillating part of Equation 13 becomes frequency-dependent. The limiting values of the amplitude are

$$A = \begin{cases} A_{\text{hf}} = \epsilon^2 C_A^3 / 4 (C_A^2 - C_\infty^2) & \text{for } \omega |\tau_V| \gg 1, \\ A_{\text{lf}} = \epsilon^2 C_A^3 / 4 (C_A^2 - C_0^2) & \text{for } \omega |\tau_V| \ll 1. \end{cases} \tag{14}$$

In the isentropically stable medium, where $C_\infty^2 > C_0^2$, there will be monotonic decay of the velocity amplitude A with respect to period from A_{hf} to A_{lf} . Such dependence will lead to a better generation of longitudinal oscillations with shorter periods. In the case of isentropic instability, there will be monotonic growth from A_{hf} to A_{lf} .

The last, but not the least, feature is appearance of the frequency-dependency velocity phase shift ϕ_0 . The maxima of the induced flow is no longer in phase with the Alfvén wave maxima. The maximum induced perturbation overtakes the Alfvén wave maximum in the isentropically stable plasma and falls behind

in the isentropically unstable plasma. As a result, the Alfvén wave steepening is modified. The greatest phase-shift is for the Alfvén wave period $P_{\max} = 4\pi\tau_V \sqrt{(C_A^2 - C_\infty^2) / (C_A^2 - C_0^2)}$. Interestingly, in the case of low plasma- β , where we have $C_A^2 \gg C_\infty^2, C_0^2$, the solution expressed by Equation 13 transfers to the solution for ideal plasma conditions (McLaughlin, de Moortel, and Hood, 2011).

3.1. Frequency Dependence of Amplitude and Phase Shift

In order to illustrate the frequency dependence of the velocity amplitude and phase shift, we use $n_0 = 10^{10} \text{ cm}^{-3}$, $T_0 = 10^6 \text{ K}$, $B_0 = 7 \text{ G}$. Also, we assume that the relative amplitude of the Alfvén wave is $\epsilon = 0.01$. In this study, the loss term due to the optically thin radiation is taken as of the form

$$L(\rho, T) = \frac{\rho}{4m^2} \Lambda(T), \quad (15)$$

where $m = 0.6 \times 1.67 \times 10^{-24} \text{ g}$ is the mean particle mass and $\Lambda(T)$ is the radiative loss function determined from the CHIANTI atomic database v. 10.0 (Dere, K. P. et al., 1997; Del Zanna et al., 2021). The heating function $H(\rho, T)$ can be locally modeled as

$$H(\rho, T) = h\rho^a T^b, \quad (16)$$

where h , a , and b are constants. The first constant h is determined from the steady-state condition $Q(\rho_0, T_0) = 0$: $h = L(\rho_0, T_0) / \rho_0^a T_0^b$. The power-law indices a and b are associated with a specific heating mechanism. In the present study we follow Kolotkov, Duckenfield, and Nakariakov (2020) and Duckenfield, Kolotkov, and Nakariakov (2021) and use the values of $a = 1/2$, $b = -7/2$, for which thermal misbalance leads to additional damping of all compressional eigenmodes.

Figure 1 demonstrates the dependence of the relative amplitude $[A/C_A]$ of the oscillating part of the longitudinal motion on the Alfvén wave period for the plasma parameters considered. It can be clearly seen that the amplitude monotonically decreases with period. Nevertheless, the absolute value of the difference between high-frequency and low-frequency amplitude limits A_{hf} and A_{lf} (Equation 14) is small. This is primarily due to the choice for the relative amplitude of the Alfvén wave [$\epsilon = 0.01$] and also due to consideration of the previously mentioned heating mechanism $[H(\rho, T) \approx \rho^{\frac{1}{2}} T^{-\frac{7}{2}}]$. The greater difference between A_{hf} and A_{lf} can be reached first by choosing of the higher relative amplitude ϵ . Furthermore, one may also consider alternative heating mechanisms contributing to greater dispersion (greater difference between C_0^2 and C_∞^2) and also the different values of magnetic field, which will lead to changes in denominators of A_{hf} and A_{lf} (Equation 14). Figure 2 illustrates dependence of the phase shift $[\phi_0]$ of the oscillating part of longitudinal motions on the Alfvén wave period. The oscillating part of the considered case is the phase shift with maximum shift at $P_{\max} = 945$ seconds for the chosen heat-loss model and specific combination of the plasma parameters. Variation in heat-loss model will lead to the variation in P_{\max} .

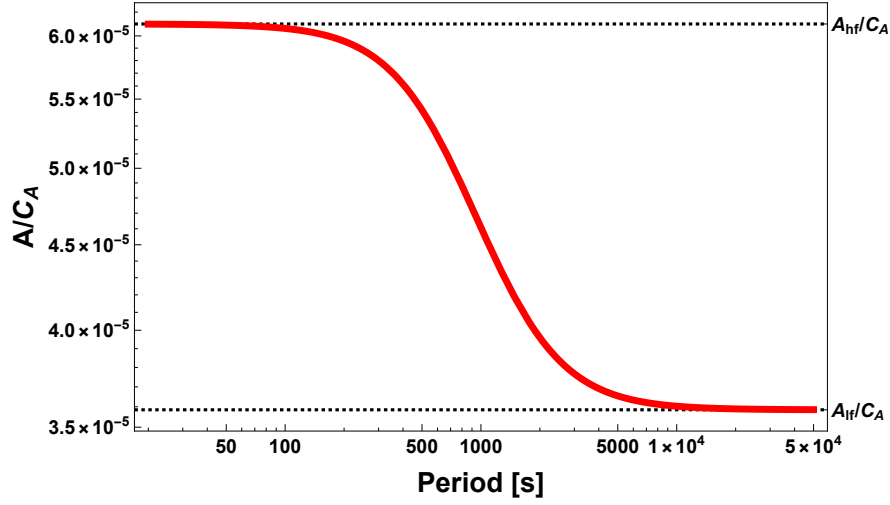


Figure 1. Dependence of the relative amplitude of the oscillating part connected with longitudinal motions induced by the Alfvén wave on the Alfvén wave period for $T_0 = 1$ MK, $n_0 = 10^{10} \text{ cm}^{-3}$ and $B_0 = 7$ G.

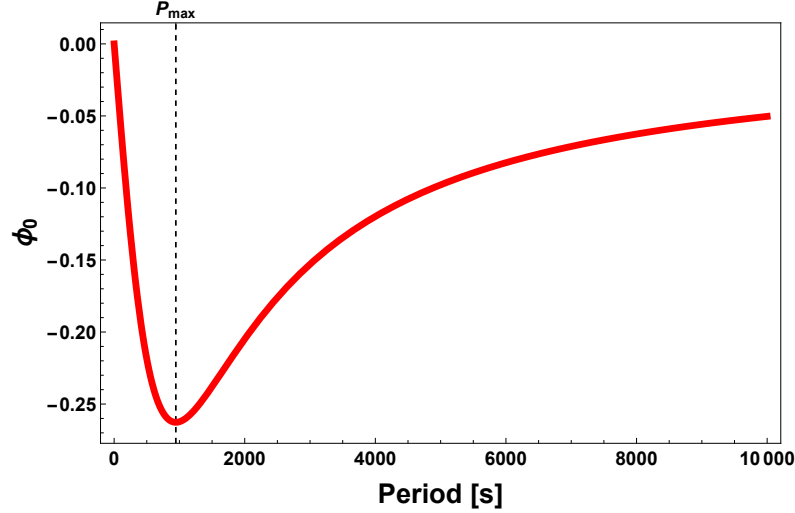


Figure 2. Dependence of the phase shift (with respect to the case of ideal plasma) of the oscillating part connected with longitudinal motions induced by the Alfvén wave on the Alfvén wave period for $T_0 = 1$ MK, $n_0 = 10^{10} \text{ cm}^{-3}$ and $B_0 = 7$ G.

3.2. Comparison with Numerical Simulations

In order to validate the analytical conclusions regarding the thermal misbalance influence on longitudinal plasma motions induced by Alfvén waves, Equations 1 – 6 have been solved numerically in 1D using the flux-corrected transport technique (Boris and Book, 1973; Toth and Odstrcil, 1996). An Alfvén wave has been

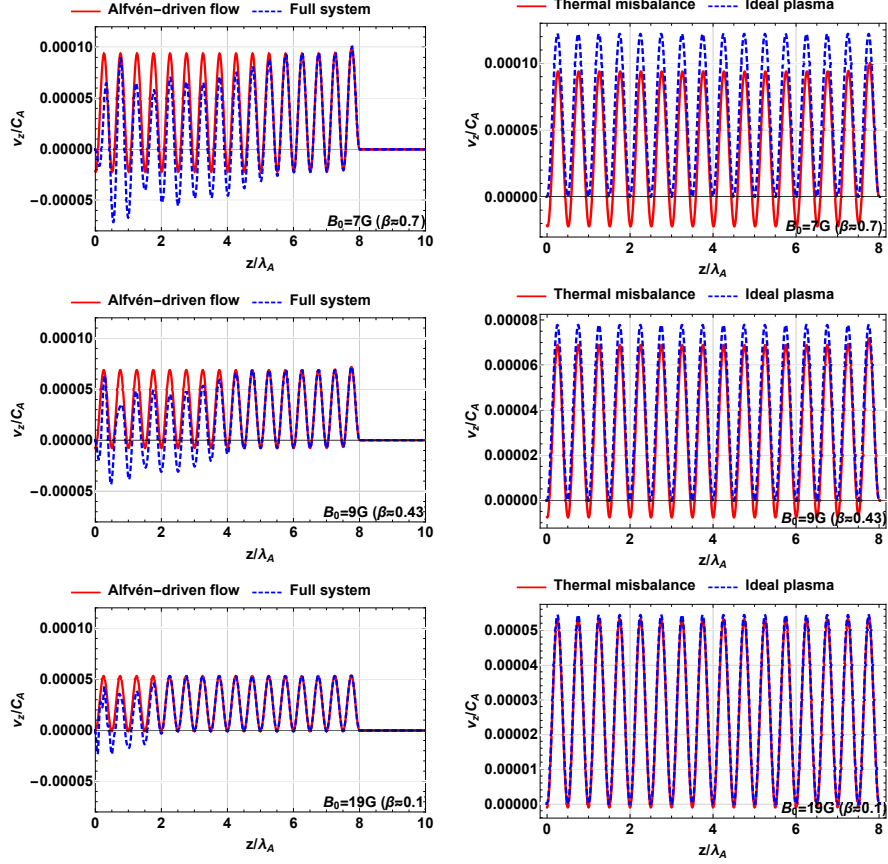


Figure 3. Relative longitudinal plasma velocity for $T_0 = 1$ MK, $n_0 = 10^{10} \text{ cm}^{-3}$, and $B_0 = 7$ G, 9 G, 19 G. *Left panel*, comparison between the analytical solution for Alfvén-induced longitudinal motions (Equation 13) and numerical solution of the full MHD system (Equations 1–6) in 1D. *Right panel*, comparison between analytical solutions for Alfvén-induced longitudinal motions in plasma with thermal misbalance and ideal plasma conditions.

generated at the left boundary of the numerical domain in the form

$$B_x = \epsilon B_0 \sin\left(\frac{2\pi}{P}t\right), \quad v_x = -\frac{B_x}{\sqrt{4\pi\rho_0}}.$$

We have chosen $\epsilon = 0.01$ and $P = 300$ seconds for the simulations. Other variables have been kept at their initial values at the left and right boundaries of the numerical domain.

The left panel of Figure 3 presents a comparison between the analytical solution for Alfvén-induced longitudinal motions obtained by Equation 13 and the numerical solution of the full 1D-MHD system obtained from Equations 1–6. It can be noticed that the numerical solution regarding the full system is constituted by two parts: acoustic perturbations and Alfvén-driven compressional perturbations. These perturbations are analytically described for plasmas

without thermal misbalance (McLaughlin, de Moortel, and Hood, 2011). When the Alfvén speed exceeds the sound speed, two domains are observed. In the right domain, only the Alfvén-driven perturbations occur which are obtained from the analytical solution expressed by Equation 13 that coincides well with the numerical solution. In the left domain, the acoustic and Alfvén-driven compressional perturbations are both present, which enables them to interact with each other. It should be mentioned that in contrast to the driven perturbation, the acoustic perturbation decays due to the chosen heating mechanism $H(\rho, T) \sim \rho^{\frac{1}{2}} T^{-\frac{7}{2}}$. Due to the simultaneous presence of the acoustic and Alfvén-driven perturbations, the numerical solution in this domain deviates from the analytical solution expressed by Equation 13 which describes Alfvén-driven perturbations only. The right panels of Figure 3 compare analytical solutions for Alfvén-induced longitudinal motions in plasmas with the thermal misbalance and in ideal plasma conditions. Firstly, it can be noticed that the solutions almost coincide for the low plasma- β conditions. It could also be noticed that the peaks of the curves ‘float up’ when thermal misbalance is present. This could be explained due to the appearance of exponential bulk flows, see the first term of Equation 13. Because of the heat-loss model and plasma parameters considered here, this flow decays rapidly from the wave front that is why only one peak is noticeably seen to ‘float up’. The ‘floating up’ signatures become weaker for lower plasma- β values. Another aspect of longitudinal motions when thermal misbalance comes in to play is the formation of areas with negative longitudinal plasma speeds. The reason for this is that the absolute value of the amplitude $[A]$ in Equation 13 is greater than the absolute value of V_0 . This is while a smaller amplitude together with a smaller negative phase shift is observed, which is presented by comparison with the oscillating part of the motion in ideal plasma conditions, see Figure 3. It is worth noting that this feature disappears for lower plasma- β conditions. The seismological aspect of the right panels of Figure 3 is associated with a change in longitudinal velocity in the presence of thermal misbalance, which is over 30 percent of the velocity amplitude for plasma- β values around 0.7 which corresponds to the solar chromosphere and corona. This could be a new seismological tool for making constraints on the solar coronal heating function using the line-of-sight velocity observations like one made by Banerjee, Pérez-Suárez, and Doyle (2009) where line-of-sight velocity increase of about 50 % was observed for coronal holes.

4. Conclusions

In this study, the effects connected with the thermal misbalance caused by longitudinal plasma motions induced by shear Alfvén waves have been analyzed. By implementing the MHD set of equations and by considering the misbalance between the energy gain and losses in the energy, of, state equation, an equation that describes the role of the thermal misbalance on the induced longitudinal flows is presented (see Equation 7). The analytical solution expressed by Equation 10 sheds light on the features imposed by thermal misbalance on the induced longitudinal plasma motions due to shear Alfvén waves. The conclusions are summarized as

- i) The observed exponential bulk flow itself modifies the Alfvén-induced plasma motions. This bulk flow arises due to the fact that the thermal misbalance causes local increase/decrease in temperature, which leads to the increase in the pressure gradients that drive bulk flows. For the case where visco-resistivity is present, the same phenomena is experienced. But in the thermally active plasmas the flow may either travel in the same direction as the Alfvén wave or travel opposite to it. The flow is co-directed with the Alfvén wave in the isentropically stable plasma ($C_\infty^2 > C_0^2$ and $\tau_V > 0$) and oppositely-directed in the isentropically unstable plasma ($C_\infty^2 < C_0^2$ and $\tau_V > 0$).
- ii) The Alfvén wave induces the longitudinal plasma motions, which causes the thermal misbalance leading to additional plasma heating or cooling. Subsequently, this heating/cooling introduces gas-dynamic pressure gradients driving longitudinal plasma motions that accelerate along the magnetic field. A simple mechanical analogue of this process is driven oscillations of a pendulum with a positive/negative friction. The external force with its own frequency moves a pendulum, but a positive/negative friction leads to the energy dissipation/gain that causes the oscillations to experience a phase shift. Based on this analogy, plasma particles act like a pendulum where the Alfvén-wave ponderomotive force is an external force while the thermal misbalance plays the role of either positive or negative friction.
- iii) In particular, the amplitude and the phase shift of the oscillating part of longitudinal plasma motion induced by shear Alfvén waves becomes frequency-dependent. This feature has been investigated analytically in application to coronal conditions. The heating mechanism considered corresponds to the isentropically stable plasma (Kolotkov, Duckenfield, and Nakariakov, 2020). We note that the amplitude dependence is a monotonic function of the wave period (frequency) with maximum values in the high-frequency interval. At the same time, the negative phase shift (Figure 2) is non-monotonic with a maximum observed at 945 seconds for the chosen heat-loss model and specific combination of the plasma parameters.

We have demonstrated that longitudinal plasma motions induced by shear Alfvén waves are affected by the thermal misbalance. This may contribute towards explaining the velocity shifts observed for propagating Alfvén waves, for instance in coronal holes, reported to be about 50 % of the amplitude (Banerjee, Pérez-Suárez, and Doyle, 2009) and constraining the coronal-heating function. This provides a basis for taking a further step to shed light on how the torsional Alfvén wave acts as a driver for longitudinal plasma motions in the presence of thermal misbalance, which will provide insight on the influence of the heating and cooling effects on the interplay of the nonlinear forces connected with the torsional Alfvén wave in the context of coronal heating.

Acknowledgments The study was supported in part by the Ministry of Education and Science of Russia by State assignment to educational and research institutions under Project No. FSSS-2020-0014 and No. 0023-2019-0003, and by RFBR, project number 20-32-90018. CHIANTI is a collaborative project involving George Mason University, the University of Michigan (USA), University of Cambridge (UK) and NASA Goddard Space Flight Center (USA).

Disclosure of Potential Conflicts of Interest The authors declare that they have no conflicts of interest. [Edit as appropriate.]

References

- Alfvén, H.: 1942, Existence of Electromagnetic-Hydrodynamic Waves. *Nature* **150**, 405. DOI. ADS.
- Antolin, P.: 2020, Thermal instability and non-equilibrium in solar coronal loops: from coronal rain to long-period intensity pulsations. *Plasma Phys and Controlled Fus* **62**, 014016. DOI. ADS.
- Banerjee, D., Pérez-Suárez, D., Doyle, J.G.: 2009, Signatures of Alfvén waves in the polar coronal holes as seen by EIS/Hinode. *Astron. Astrophys.* **501**, L15. DOI. ADS.
- Belov, S., Molevich, N., Zavershinskii, D.: 2019a, Propagation of nonlinear alfvén waves in heat-releasing plasma. *Phys Scr* **94**, 105605. DOI. <https://doi.org/10.1088/1402-4896/ab2f02>.
- Belov, S., Molevich, N., Zavershinskii, D.: 2020, Thermal Misbalance Influence on the Nonlinear Shear Alfvén Waves Under Solar Atmosphere Conditions. *Solar Phys.* **295**, 160. DOI. ADS.
- Belov, S.A., Molevich, N.E., Zavershinskii, D.I.: 2018, Amplification of Alfvén Waves due to Nonlinear Interaction with a Fast Magnetoacoustic Wave in Acoustically Active Conductive Media. *Tech Phys Lett* **44**, 199. DOI. ADS.
- Belov, S.A., Molevich, N.E., Zavershinskii, D.I.: 2019b, Alfvén Wave Amplification as a Result of Parametric Quasi-Resonant Interaction with Magnetoacoustic Waves in Heat-Releasing Isentropically Unstable Plasma. *Russ Phys J* **62**, 179. DOI. ADS.
- Boris, J.P., Book, D.L.: 1973, Flux-corrected transport. i. shasta, a fluid transport algorithm that works. *J Comp Phys* **11**, 38. DOI.
- Chin, R., Verwichte, E., Rowlands, G., Nakariakov, V.M.: 2010, Self-organization of magnetoacoustic waves in a thermally unstable environment. *Physics of Plasmas* **17**, 032107. DOI. ADS.
- Claes, N., Keppens, R.: 2019, Thermal stability of magnetohydrodynamic modes in homogeneous plasmas. *Astron. Astrophys.* **624**, A96. DOI. ADS.
- Craig, I.J.D., Fruit, G.: 2005, Wave energy dissipation by phase mixing in magnetic coronal plasmas. *Astron. Astrophys.* **440**, 357. DOI. ADS.
- Del Zanna, G., Dere, K.P., Young, P.R., Landi, E.: 2021, CHIANTI—An Atomic Database for Emission Lines. XVI. Version 10, Further Extensions. *Astrophys. J.* **909**, 38. DOI. ADS.
- Dere, K. P., Landi, E., Mason, H. E., Monsignori Fossi, B. C., Young, P. R.: 1997, Chianti - an atomic database for emission lines* - i. wavelengths greater than 50 Å. *Astron. Astrophys. Suppl. Ser.* **125**, 149. DOI.
- Duckenfield, T.J., Kolotkov, D.Y., Nakariakov, V.M.: 2021, The effect of the magnetic field on the damping of slow waves in the solar corona. *Astron. Astrophys.* **646**, A155. DOI. ADS.
- Farahani, S.V., Hejazi, S.M., Boroomand, M.R.: 2021, Torsional Alfvén Wave Cascade and Shocks Evolving in Solar Jets. *Astrophys. J.* **906**, 70. DOI. ADS.
- Field, G.B.: 1965, Thermal Instability. *Astrophys. J.* **142**, 531. DOI. ADS.
- Kolotkov, D.Y., Duckenfield, T.J., Nakariakov, V.M.: 2020, Seismological constraints on the solar coronal heating function. *Astron. Astrophys.* **644**, A33. DOI.
- Kolotkov, D.Y., Nakariakov, V.M., Zavershinskii, D.I.: 2019, Damping of slow magnetoacoustic oscillations by the misbalance between heating and cooling processes in the solar corona. *Astron. Astrophys.* **628**, A133. DOI. ADS.
- McLaughlin, J.A., de Moortel, I., Hood, A.W.: 2011, Phase mixing of nonlinear visco-resistive Alfvén waves. *Astron. Astrophys.* **527**, A149. DOI. ADS.
- Molevich, N.: 2001, Excitation of the opposite acoustic flows in thermodynamically nonequilibrium gaseous media. *Tech Phys Lett* **27**, 900.
- Molevich, N.: 2002, Nonstationary self-focusing of sound beams in a vibrationally excited molecular gas. *Acoustical Physics* **48**, 209.
- Molevich, N.E., Oraevskii, A.N.: 1988, Second viscosity in thermodynamically nonequilibrium media. *Zh. Eksp. Teor. Fiz* **94**, 128. [J. Exp. Theor. Phys. **67**, 504 (1988)].
- Mozafari Ghoraba, A., Vasheghani Farahani, S.: 2018, Properties of Nonlinear Torsional Waves Effective on Solar Swirling Plasma Motions. *Astrophys. J.* **869**, 93. DOI. ADS.
- Nakariakov, V.M., Roberts, B., Murawski, K.: 1997, Alfvén Wave Phase Mixing as a Source of Fast Magnetosonic Waves. *Solar Phys.* **175**, 93. DOI. ADS.

- Nakariakov, V.M., Afanasyev, A.N., Kumar, S., Moon, Y.-J.: 2017, Effect of Local Thermal Equilibrium Misbalance on Long-wavelength Slow Magnetoacoustic Waves. *Astrophys. J.* **849**, 62. DOI. ADS.
- Parker, E.N.: 1953, Instability of Thermal Fields. *Astrophys. J.* **117**, 431. DOI. ADS.
- Prasad, A., Srivastava, A.K., Wang, T.J.: 2021, Role of Compressive Viscosity and Thermal Conductivity on the Damping of Slow Waves in Coronal Loops with and Without Heating-Cooling Imbalance. *Solar Phys.* **296**, 20. DOI. ADS.
- Priest, E.: 2014, *Magnetohydrodynamics of the Sun*, Cambridge University Press. DOI. ADS.
- Prokopyshyn, A.P.K., Hood, A.W., De Moortel, I.: 2019, Phase mixing of nonlinear Alfvén waves. *Astron. Astrophys.* **624**, A90. DOI. ADS.
- Ruderman, M.S., Petrukhin, N.S.: 2018, Phase mixing of Alfvén waves in two-dimensional magnetic plasma configurations with exponentially decreasing density. *Astron. Astrophys.* **620**, A44. DOI. ADS.
- Sabri, S., Vasheghani Farahani, S., Ebadi, H., Hosseinpour, M., Fazel, Z.: 2018, Alfvén wave dynamics at the neighbourhood of a 2.5D magnetic null-point. *Mon. Not. Roy. Astron. Soc.* **479**, 4991. DOI. ADS.
- Sabri, S., Farahani, S.V., Ebadi, H., Poedts, S.: 2020, How Alfvén waves induce compressive flows in the neighborhood of a 2.5D magnetic null-point. *Sci Rep* **10**, 15603. DOI. ADS.
- Shestov, S.V., Nakariakov, V.M., Ulyanov, A.S., Reva, A.A., Kuzin, S.V.: 2017, Nonlinear Evolution of Short-wavelength Torsional Alfvén Waves. *Astrophys. J.* **840**, 64. DOI. ADS.
- Srivastava, A.K., Shetye, J., Murawski, K., Doyle, J.G., Stangalini, M., Scullion, E., Ray, T., Wójcik, D.P., Dwivedi, B.N.: 2017, High-frequency torsional Alfvén waves as an energy source for coronal heating. *Sci Rep* **7**, 43147. DOI. ADS.
- Srivastava, A.K., Murawski, K., Kuźma, B., Wójcik, D.P., Zaqarashvili, T.V., Stangalini, M., Musielak, Z.E., Doyle, J.G., Kayshap, P., Dwivedi, B.N.: 2018, Confined pseudo-shocks as an energy source for the active solar corona. *Nature Astron* **2**, 951. DOI. ADS.
- Thurgood, J.O., McLaughlin, J.A.: 2013, Nonlinear Alfvén wave dynamics at a 2D magnetic null point: ponderomotive force. *Astron. Astrophys.* **555**, A86. DOI. ADS.
- Toth, G., Odstrčil, D.: 1996, Comparison of some flux corrected transport and variation diminishing numerical schemes for hydrodynamic and magnetohydrodynamic problems. *J Comp Phys* **128**, 82. DOI.
- Vasheghani Farahani, S., Hejazi, S.M.: 2017, Coronal Jet Collimation by Nonlinear Induced Flows. *Astrophys. J.* **844**, 148. DOI. ADS.
- Vasheghani Farahani, S., Nakariakov, V. M., Van Doorselaere, T., Verwichte, E.: 2011, Nonlinear long-wavelength torsional alfvén waves. *Astron. Astrophys* **526**, A80. DOI.
- Verwichte, E., Nakariakov, V.M., Longbottom, A.W.: 1999, On the evolution of a nonlinear Alfvén pulse. *J Plasma Phys* **62**, 219. DOI. ADS.
- Zavershinskii, D.I., Kolotkov, D.Y., Nakariakov, V.M., Molevich, N.E., Ryashchikov, D.S.: 2019, Formation of quasi-periodic slow magnetoacoustic wave trains by the heating/cooling misbalance. *Phys Plasmas* **26**, 082113. DOI.
- Zavershinskii, D.I., Molevich, N.E., Riashchikov, D.S., Belov, S.A.: 2020, Nonlinear magnetoacoustic waves in plasma with isentropic thermal instability. *Phys. Rev. E* **101**, 043204. DOI.
- Zavershinskiy, D.I., Molevich, N.E.: 2015, Parametrical amplification of Alfvén waves in heat-releasing ionized media with magnetoacoustic instability. *Astrophys. Space Sci.* **358**, 22. DOI. ADS.